

Proteome Interrogation Using Nanoprobes To Identify Targets of a Cancer-Killing Molecule

Liwen Li,[†] Qiu Zhang,[†] Aifeng Liu,[†] Xiue Li,[†] Hongyu Zhou,[‡] Yin Liu,[†] and Bing Yan^{*,†,‡}[†]Key Laboratory of Colloid and Interface Chemistry of the Ministry of Education, School of Chemistry and Chemical Engineering, Shandong University, Jinan 250100, China[‡]Department of Chemical Biology and Therapeutics, St. Jude Children's Research Hospital, Memphis, Tennessee 38105, United States

Supporting Information

ABSTRACT: We report a generic approach for identification of target proteins of therapeutic molecules using nanoprobes. Nanoprobes verify the integrity of nanoparticle-bound ligands in live cells and pull down target proteins from the cellular proteome, providing very important information on drug targets and mechanisms of action. As an example, target proteins as α -tubulin and HSP 90 have been identified and validated.

Devastating diseases such as central nervous system disorders and cancer are complex diseases that can result from multiple genetic mutations. In the search for new treatments, simple approaches such as single-target protein screenings often fail to yield innovative drugs. In contrast, multitargeting molecules are often advantageous in the treatment of these complex diseases because they affect multiple pathways.^{1,2} Drug resistance is also less likely to develop with these molecules.[†] However, multitargeting drugs are difficult to discover through rational drug design or single-protein screening approaches. Phenotype screening and optimization are promising methods for developing such therapeutics, provided that the targets and mechanisms of action can be elucidated to show the therapeutic and side effects of the drugs and develop second-generation drugs with a better profile.

Affinity methods, which are often used in target identification, use a solid support that attaches active compounds to pull down proteins after incubation with cell lysate.^{3–6} Bound proteins are separated by sodium dodecyl sulfate polyacrylamide gel electrophoresis (SDS-PAGE), and then their identities are determined. However, a major drawback of these methods is that it is not possible to confirm whether the target-binding specificity is altered by chemical modification and the linkage to the solid support because of the large size of testing beads.

Nanoparticles with bioactive compounds on the surface can enter live cells to confirm the desired biological activity and targeting specificity of the modified compound and at the same time identify target proteins by interrogating the cellular proteome in cell lysate. To test this hypothesis, we designed and synthesized compound **1** (Figure 1). Compound **1** selectively killed nonsmall cell lung cancer H460 cells with a median effective concentration (EC_{50}) of 0.9 μ M and was much less toxic to normal human fibroblasts ($EC_{50} > 100 \mu$ M). However, its primary targets and mechanisms of action are not known.⁷ Compound **3** is a structural

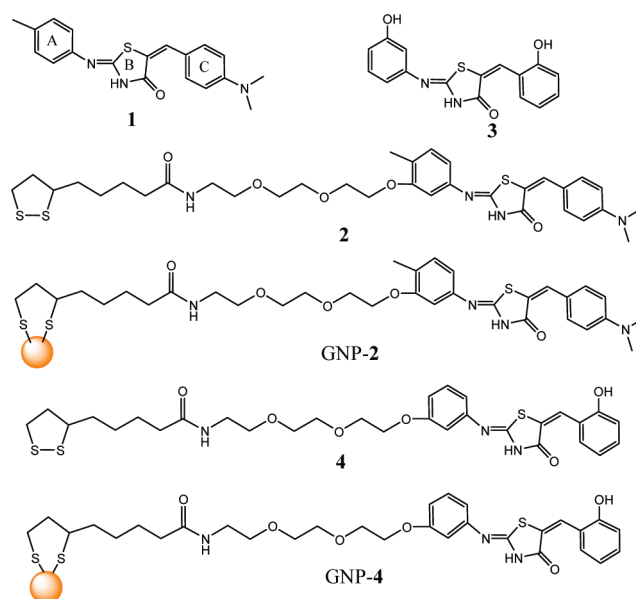


Figure 1. Structure of **1** and **3**, their derivative **2** and **4**, GNP-2 and GNP-4.

analogue of compound **1**, it was much less toxic to H460 ($EC_{50} = 53.7 \mu$ M).

Previous structure–activity relationship studies showed that rings B and C in **1** are stereochemically confined, while ring A is much more tolerant of structural modifications. We modified ring A [Scheme S1 in the Supporting Information (SI)] by attaching a flexible and biocompatible linker to give compound **2**, and a similar modification of **3** gave **4**. GNP-2 and GNP-4 (Figure 1) were then synthesized in situ using a reported method⁸ (see the SI for detailed syntheses and characterizations of GNP-2 and GNP-4). GNP-4 derived from inactive compound **3** was used as a control (Figure 1) for target validation.

High-resolution transmission electron microscopy (TEM) analysis (Figure 2a,b) showed that the average diameter of the GNP-2 particles was 2.5 nm (Figure 2b). The GNP-linked ligands were analyzed by high-performance liquid chromatography/mass spectrometry (HPLC/MS) after cleavage with I_2 . The chromatogram (Figure 2c) and the associated electrospray ionization MS (ESI-MS) spectrum (Figure 2d) showed that the peak at 6.6 min corresponded to compound **2** (MW 672.25).

Received: December 14, 2010

Published: April 15, 2011

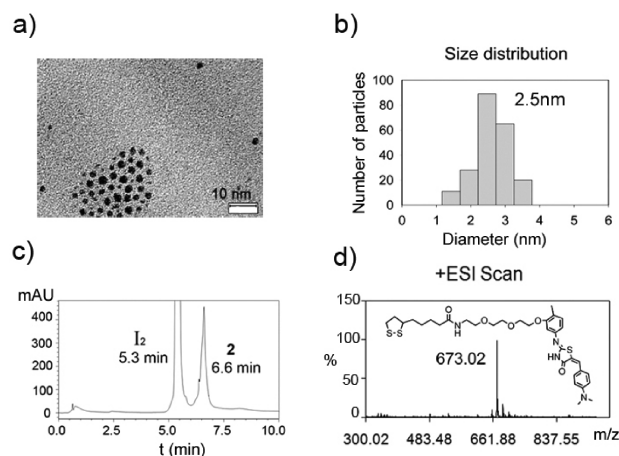


Figure 2. (a, b) Characterization of GNP-2: (a) TEM image of GNP-2. Scale bar = 10 nm. (b) Size distribution of GNP-2 according to TEM images. The average diameter was 2.5 nm. (c, d) Structure identification of free ligands cleaved from GNP-2 by I_2 : (c) Chromatogram. The peak at 5.3 min is I_2 , and the peak at 6.6 min is compound 2. (d) ESI-MS spectrum corresponding to the peak at 6.6 min.

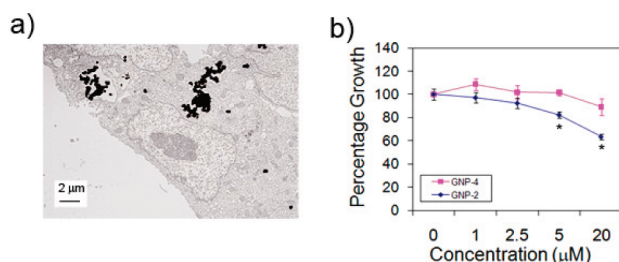


Figure 3. (a) TEM image of GNP-2 cell uptake. H460 cells were treated with 5 μ M GNP-2 for 48 h. Scale bar = 2 μ m. (b) Percentage growth of H460 cells treated with GNP-2 and GNP-4 for 48 h. The concentrations of GNP-2 and GNP-4 were 0, 1, 2.5, 5, and 20 μ M. Results represent mean \pm standard error of the mean (SEM) in triplicate. The * label indicates that the percentage growth of the group treated with GNP-2 was significantly different ($P < 0.05$) from that of the group treated with GNP-4 under the same conditions.

On average, there were ~ 65 ligands on each GNP (see section 4 in the SI). Since the chemical modifications and the attachment to a GNP might alter the target-binding specificity, it was necessary to test whether GNP-2 could still enter and kill cancer cells. Figure 3a shows that GNP-2 particles could readily enter cells. Although some GNP-2 particles were found in the cytoplasm, most of them were in endosomes. The cytotoxicity results (Figure 3b) showed that GNP-2 exhibited dose-dependent toxicity toward H460 cells, but GNP-4 showed much less toxicity. Because GNP-2 particles were mainly trapped in endosomes, as most nanoparticles are, the reduced cytoplasm entry might have been responsible for a higher EC_{50} value than for the free compound 1. However, GNP-2 maintained its target-binding and anticancer activities. Although the protein pulled down with this method was eventually validated by a series of biological studies, this nanoparticle-based prequalification assay in live cells provided key guidance at a very early stage.

After they were proven to be active in live cells, GNP-2 and GNP-4 were incubated with cancer cell lysate for 1 h before the bound proteins were separated and analyzed by electrophoresis.

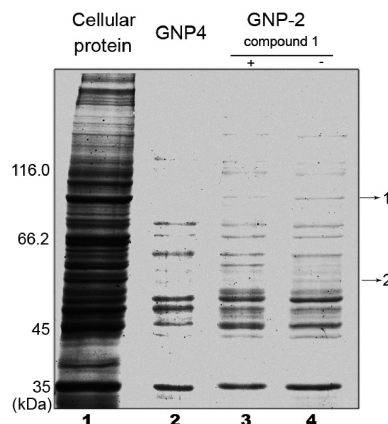


Figure 4. Target identification by GNP-2. H460 cell extract (300 μ L) was incubated with (lane 3) or without (lane 4) 5 mM compound 1 for 1 h at 4 $^{\circ}$ C, after which 0.03 μ mol of GNP-2 was added and the mixture incubated for 1 h at 4 $^{\circ}$ C. As a control, cell extract (300 μ L) was also incubated with GNP-4 and treated in the same way (lane 2). Proteins bound to GNPs were separated by 10% SDS-PAGE followed by improved Coomassie brilliant blue G-250 staining.¹⁴ Protein bands with lower intensities in the lane with compound 1 than in the lane without compound 1 were identified by MALDI-TOF/TOF MS and Mascot analysis (Table 1).

Table 1. Protein Identification by MALDI-TOF/TOF MS and Mascot Analysis

band	protein	gene	protein score CI (%) ^a
1	heat shock protein HSP 90- β	Hsp90ab1	100
2	tubulin α -1 C chain	TUBA1C	100

^aThe protein score confidence interval (CI) was calculated using the Mascot search engine to assess the match between the experimental data and the database sequence.

More than 10 protein bands ranging from 35 to 150 kDa were observed for GNP-2 (lane 4), while fewer proteins were seen for GNP-4 (lane 2). To ensure that only proteins with specific binding to GNP-2 were correctly identified, we also preincubated compound 1 with the lysate for 1 h at 4 $^{\circ}$ C and then incubated this cell lysate with GNP-2 for an additional 1 h (lane 3). Comparison of lane 4 with lanes 3 and 2 revealed that only two protein bands showed reduced intensities (Figure 4), indicating that they might be the specific target proteins of compound 1. The identities of these proteins were determined by matrix-assisted laser desorption ionization tandem time-of-flight (MALDI-TOF/TOF) MS and data analysis using the Mascot search engine (Table 1). Protein identification results with a protein score confidence interval of 100% were accepted. These proteins were heat shock protein 90- β (β -HSP 90) and tubulin α -1C chain. The proteins α -tubulin⁹⁻¹¹ and β -HSP 90^{12,13} are validated therapeutic targets for cancer treatment. Thus, α -tubulin and β -HSP 90 could be considered as the potential targets of compound 1.

Among target proteins of compound 1, tubulin is a key anti-cancer target. Tubulin-binding agents can stabilize (such as paclitaxel) or destabilize (such as colchicine) microtubule formation, block cell-cycle progression, and cause apoptosis. To validate tubulin as a target for compound 1, we first investigated the compound's effect on tubulin polymerization in vitro and on

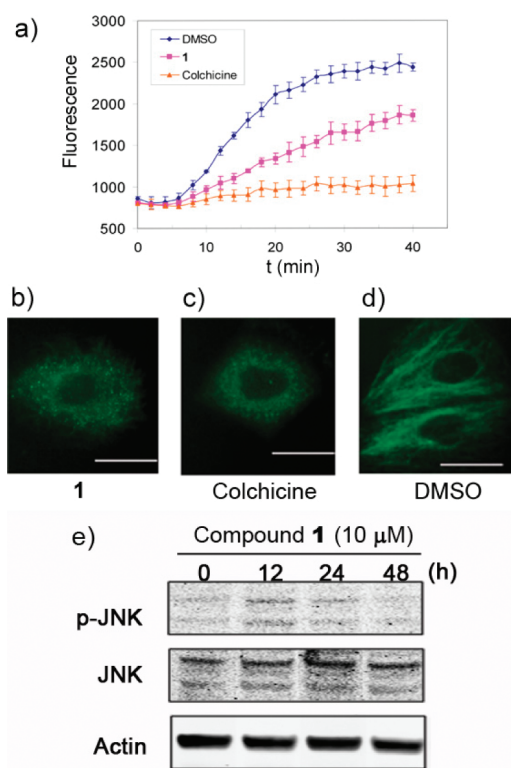


Figure 5. Validation of tubulin as a target. DMSO and colchicine were used as negative and positive controls. (a) Microtubule polymerization assay. The concentrations of compound 1 and colchicine were 10 and 5 μ M, respectively. Results represent mean \pm SEM from two independent experiments. (b–d) Microtubule immunofluorescence microscopy images of H460 cells incubated with (b) 1 μ M compound 1, (c) 1 μ M colchicine, and (d) DMSO for 24 h. Microtubules were labeled by α -tubulin antibody. Scale bar = 25 μ m. (e) Western blot analysis for p-JNK and JNK in the H460 cell extracts prepared after 0, 12, 24, and 48 h of treatment with 10 μ M compound 1.

microtubule assembly/disassembly processes in live cells. Tubulin subunits self-assemble to form cylindrical microtubules in a time-dependent manner (Figure 5a). Colchicine, a microtubule depolymerizing agent, inhibited microtubule polymerization (Figure 5a).^{15,16} Compound 1 also caused microtubule depolymerization in a manner similar to that of colchicine (Figure 5a). To substantiate this finding, compound 1's effects on microtubule organization in live cells were investigated using immunofluorescence microscopy. The microtubule network in cells treated with 1 μ M colchicine (Figure 5c) or compound 1 (Figure 5b) was disrupted completely. To further validate compound 1 as a microtubule-interfering agent, we investigated compound 1-induced activation of c-Jun NH2-terminal kinase (JNK). JNK activation is a hallmark event for microtubule-interfering agents such as paclitaxel, vinblastine, vincristine, docetaxel, and nocodazole.^{17–20} The elevated level of p-JNK by compound 1 was detected, and compound 1-induced JNK activation peaked at 12 h (Figure 5e). These results demonstrate that compound 1 inhibits microtubule organization in live cells by binding to tubulin and inhibiting its polymerization.

In cancer cells, HSP 90 is overexpressed to actively assist folding and maturation of oncogenic proteins such as CRAF-1 and ERBB2 and also to assist AKT phosphorylation. Blocking HSP 90 leads to degradation of these proteins and inhibition of

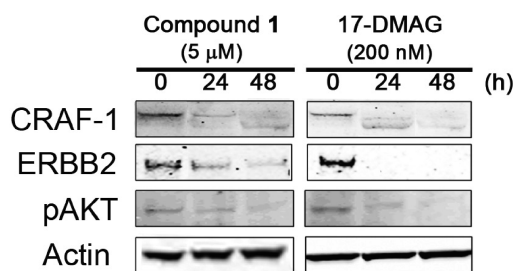


Figure 6. Validation of HSP 90 as a target through Western blot analysis for HSP 90 client proteins CRAF-1, ERBB2, and p-AKT in H460 cell extracts prepared after 0, 24, and 48 h of treatment with (left) 5 μ M compound 1 and (right) 200 nM 17-DMAG, which is a known HSP 90 inhibitor.

AKT phosphorylation.^{21–23} We investigated whether compound 1, after binding to HSP 90, inhibited its chaperone activity and caused degradation of CRAF-1 and ERBB2 and inhibition of AKT phosphorylation in comparison with a known HSP 90 inhibitor, 17-dimethylaminoethylamino-17-demethoxygeldanamycin (17-DMAG).¹² 17-DMAG inhibits HSP 90, inducing proteosome-dependent degradation of CRAF-1 and ERBB2 and inhibiting phosphorylation of AKT (Figure 6, right panels). Similar protein degradation patterns (CRAF-1 and ERBB2) were also observed for compound 1. It also induced a time-dependent inhibition of AKT phosphorylation. These results reveal that the anticancer mechanism of action of compound 1 partly involves inhibition of HSP 90 function.

After the discovery and validation that compound 1 specifically inhibits tubulin and HSP 90, the mechanism of action of this compound was further substantiated by its role in inducing G2/M cell-cycle arrest and apoptosis (Figure S5 in the SI).

In summary, we have used nanoprobe to identify dual targets for compound 1 in this work by first validating its anticancer activity in live cells and then interrogating the proteome in cell lysate. Our findings demonstrate the power of nanotechnology in drug discovery and chemical biology research. Target identification for therapeutic compounds has been a severely underdeveloped area in drug discovery research, and the validation of uncertain targets is tedious and expensive. Nanoprobes will likely play a pivotal role in this area.

■ ASSOCIATED CONTENT

S Supporting Information. Details of the synthesis of compound 2, quantification of the ligand contents of GNP-2, cell-cycle arrest and apoptosis induced by compound 1, experimental procedures, and complete refs 3 and 5. This material is available free of charge via the Internet at <http://pubs.acs.org>.

■ AUTHOR INFORMATION

Corresponding Author
dr.bingyan@gmail.com

■ ACKNOWLEDGMENT

This work was supported by the National Basic Research Program of China (2010CB933504), the National Natural Science Foundation of China (90913006 and 21077068), the National Cancer Institute (P30CA027165), the American Lebanese

Syrian Associated Charities (ALSAC), and St. Jude Children's Research Hospital. We thank Dr. Vishwajeeth Reddy Pagala and Ms. Linda Mann for technical assistance.

REFERENCES

- (1) Frantz, S. *Nature* **2005**, *437*, 942.
- (2) Roth, B. L.; Sheffler, D. J.; Kroeze, W. K. *Nat. Rev. Drug Discovery* **2004**, *3*, 353.
- (3) Bach, S.; et al. *J. Biol. Chem.* **2005**, *280*, 31208.
- (4) Leslie, B. J.; Hergenrother, P. J. *Chem. Soc. Rev.* **2008**, *37*, 1347.
- (5) Shimizu, N.; et al. *Nat. Biotechnol.* **2000**, *18*, 877.
- (6) von Rechenberg, M.; Blake, B. K.; Ho, Y. S. J.; Zhen, Y. J.; Chepanoske, C. L.; Richardson, B. E.; Xu, N. F.; Kery, V. *Proteomics* **2005**, *5*, 1764.
- (7) Zhou, H. Y.; Wu, S. H.; Zhai, S. M.; Liu, A. F.; Sun, Y.; Li, R. S.; Zhang, Y.; Ekins, S.; Swaan, P. W.; Fang, B. L.; Zhang, B.; Yan, B. *J. Med. Chem.* **2008**, *51*, 1242.
- (8) Zhou, H. Y.; Du, F. F.; Li, X.; Zhang, B.; Li, W.; Yan, B. *J. Phys. Chem. C* **2008**, *112*, 19360.
- (9) Chang, J.-Y.; Chang, C.-Y.; Kuo, C.-C.; Chen, L.-T.; Wein, Y.-S.; Kuo, Y.-H. *Mol. Pharmacol.* **2004**, *65*, 77.
- (10) Jordan, A.; Hadfield, J. A.; Lawrence, N. J.; McGown, A. T. *Med. Res. Rev.* **1998**, *18*, 259.
- (11) Jordan, M. A.; Wilson, L. *Nat. Rev. Cancer* **2004**, *4*, 253.
- (12) Holzbeierlein, J.; Windsperger, A.; Vielhauer, G. *Curr. Oncol. Rep.* **2010**, *12*, 95.
- (13) Workman, P.; Powers, M. V. *Nat. Chem. Biol.* **2007**, *3*, 455.
- (14) Diezel, W.; Kopperschlager, G.; Hofmann, E. *Anal. Biochem.* **1972**, *48*, 617.
- (15) Garland, D. L. *Biochemistry* **1978**, *17*, 4266.
- (16) Skoufias, D. A.; Wilson, L. *Biochemistry* **1992**, *31*, 738.
- (17) Lee, L.-F.; Li, G.; Templeton, D. J.; Ting, J. P.-Y. *J. Biol. Chem.* **1998**, *273*, 28253.
- (18) Wang, T.-H.; Wang, H.-S.; Ichijo, H.; Giannakakou, P.; Foster, J. S.; Fojo, T.; Wimalasena, J. *J. Biol. Chem.* **1998**, *273*, 4928.
- (19) Mollinedo, F.; Gajate, C. *Apoptosis* **2003**, *8*, 413.
- (20) Gajate, C.; Barasoain, I.; Andreu, J. M.; Mollinedo, F. *Cancer Res.* **2000**, *60*, 2651.
- (21) Moser, C.; Lang, S. A.; Stoeltzing, O. *Anticancer Res.* **2009**, *29*, 2031.
- (22) Sain, N.; Krishnan, B.; Ormerod, M. G.; De Rienzo, A.; Liu, W. M.; Kaye, S. B.; Workman, P.; Jackman, A. L. *Mol. Cancer Ther.* **2006**, *5*, 1197.
- (23) Powers, M. V.; Workman, P. *Endocr.-Relat. Cancer* **2006**, *13*, S125.